Development and Preliminary Testing of a Mobile Robot for Cardiac Intervention

Nicholas A Patronik

CMU-RI-TR-05-08

February 2005

The Robotics Institute
Carnegie Mellon University
Pittsburgh, Pennsylvania 15213

Submitted in partial fulfillment of the requirements for the degree of Master of Science

Abstract

This report describes the development and preliminary testing of a mobile robotic device (HeartLander) to facilitate minimally invasive intervention on the beating heart. The HeartLander robot will be placed onto the surface of the heart through a port inserted below the sternum. It will then adhere to the heart surface, and under the control of the surgeon, navigate to any location to administer therapy. As compared to current robot-assisted cardiac surgery, this novel paradigm obviates immobilization of the heart and eliminates access limitations. Furthermore, HeartLander allows the use of an insertion method that could enable outpatient cardiac surgery, which is not possible using conventional minimally invasive techniques. The current prototype uses suction to maintain prehension of the heart, and wire-driven remote actuation for locomotion. A digitized fiberscope displays visual feedback to the surgeon, who controls the device through a joystick interface. The initial prototype demonstrated successful prehension, turning, and locomotion on open-chest, beating pig hearts with excised pericardiums (N=3). This work illustrates the feasibility of using a miniature mobile robot to navigate on the beating heart.

Table of Contents

1 BACKGROUND 1

1.1 CARDIAC SURGERY 1
1.1.1 Minimally Invasive Cardiac Surgery 1
1.1.2 Robot-Assisted Cardiac Surgery 1
1.1.3 Limitations of Robot-Assisted Cardiac Surgery 2
1.2 THE HEARTLANDER CONCEPT 4

2 DESIGN CONCEPTS 6

2.1 SYSTEM REQUIREMENTS 6
2.2 PREHENSION 6
2.3 ACTUATION 7
2.4 LOCOMOTION 8
2.4.1 Tank 8
2.4.2 Roller 8
2.4.3 Cartesian Walker 9
2.4.4 Polar Walker 9
2.4.5 Bending Inchworm Walker 9
2.4.6 Final Selection 10
2.5 VIDEO FEEDBACK 10

3 DESIGN IMPLEMENTATION 12

3.1 SUPPORTING INSTRUMENTATION 13
3.2 MECHANICAL TRANSMISSION 14
3.3 CRAWLER ROBOT 15
3.3.1 Construction 15
3.3.2 Kinematics 15
3.3.3 Inherent Compliance 17

4 DESIGN APPLICATION 18

4.1 INSERTION 18
4.2 LOCOMOTION 18
4.3 CONTROL 20
4.4 THERAPY 20

5 TESTING 21

5.1 BENCH TESTING 21
5.1.1 Prehensile Testing with a Poultry Model 21
5.1.2 Manual Locomotion Testing with Poultry Model 22
5.1.3 Locomotion Testing with Balloon Model 22
5.2 *IN VIVO* PORCINE TESTING 23

6 DISCUSSION AND FUTURE WORK 26

REFERENCES 27

1 Background

1.1 Cardiac Surgery

1.1.1 Minimally Invasive Cardiac Surgery

The use of minimally invasive procedures has become a major objective in the field of cardiothoracic surgery due to the desire to avoid the morbidity associated with sternotomy and cardiopulmonary bypass (Mack 2001). *Sternotomy* is the cutting of the sternum to open the ribcage, which provides direct access to the heart for the surgeon. Sternotomy is typically obviated using *endoscopic* minimally invasive surgery. This technique utilizes miniature cameras and tools located on the distal ends of rigid shafts that are inserted through small incisions made between the ribs (Figure 1). Using these endoscopic instruments, the surgeon is able to bring the tools to the operative site, rather than opening the patient to expose the operative site to the tools. This greatly reduces the morbidity of surgical procedures, as the majority of the pain and disability experienced by the patient is caused by gaining access rather than the procedure itself (Mack 2001).

Despite this fact, the original handheld endoscopic instruments had several drawbacks that limited the adoption of minimally invasive techniques for many surgical procedures. These problems included: decreased dexterity, poor visualization, reduced hand-eye coordination, motion reversing, inadvertent motion scaling, and fatigue. These problems were exacerbated by the confined environment of minimally invasive surgery, and led to the exploration of robotic solutions.

1.1.2 Robot-Assisted Cardiac Surgery

In 1993, DARPA launched its Advanced Biomedical Technologies program to develop advanced healthcare solutions for combat casualties. One of the major thrusts was to develop a robotic telesurgical system through which a surgeon could perform remote surgery on a wounded soldier on the battlefield. The technology that emerged was a teleoperated workstation, where the motions of the surgeons hands on a pair of input devices was mimicked by a pair of robotic manipulators located near the patient (Bowersox 1998). Despite successful laboratory testing, the high bandwidth requirements of this system have thus far prevented its use in remote telesurgery. The technology was licensed and developed into two commercially-available robotic surgical systems for endoscopic surgery. The Da Vinci Surgical Robot (Intuitive Surgical, CA) is shown in Figure 2. The advantages for endoscopic surgery provided by these systems include:

- increased dexterity,
- high-resolution 3D stereo vision,
- restored hand-eye coordination,
- elimination of motion reversing,
- controlled motion and force scaling, and
- tremor reduction.

For these reasons, the robotic endoscopic teleoperated systems are currently used in many procedures (Diodato and Damiano 2003).

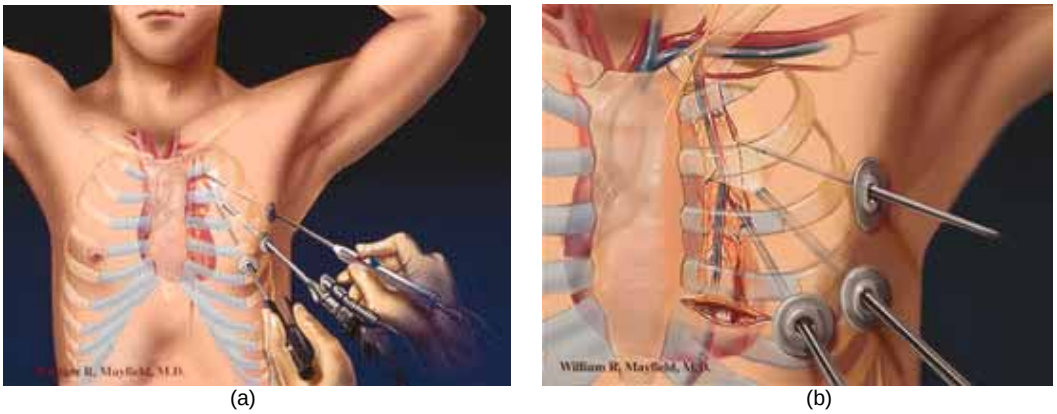

(a) (b)

Figure 1. (b) Illustration of cardiac laparoscopy using handheld instrumentation. The two outer shafts *(held by the surgeon)* are the laparoscopic tools, while the center shaft is the scope. (b) Close up of the access ports and instrumentation.

Figure 2 . The Da Vinci teleoperated robotic manipulator system. Insets show close ups of the input handles *(upper left)* and the surgical robotic manipulators *(lower right)*.

1.1.3 Limitations of Robot-Assisted Cardiac Surgery

Despite the improvements to endoscopic surgery resulting from robotic instrumentation, the teleoperated manipulator paradigm has several limitations with regards to cardiac surgery. The most significant disadvantages include:

- limited operative site selection,
- tool reinsertion required to change sites,
- lung deflation required, and
- epicardial stabilization required.

These problems have limited the incorporation of minimally invasive techniques into many cardiac procedures, and are now explained in greater detail (Diodato 2003).

The *intercostal transthoracic* approach (incisions made between the ribs to enter the chest) used for the insertion of endoscopic manipulators leads to several problems. Due to the anatomical constraints posed by the lungs, this approach can only be used to reach the anterior surface of the heart. Thus many regions of the heart cannot be accessed, such as the posterior wall of the left ventricle (Falk et al. 2000). Even for the regions of the heart that can be reached, only a small portion of the epicardial surface can be accessed from a single set of incisions. If a second operative site is desired, the tools must be extracted and reinserted through a new set of incisions. Lastly, the intercostal transthoracic approach requires that the rigid tools pass through the *pleural space* (the space naturally occupied by the lungs). This requires general anesthesia, differential lung ventilation, and deflation of the left lung to create sufficient space for the tools to safely pass by the left lung. This increases the morbidity of the procedure and requires an overnight stay in the hospital regardless of the severity of the procedure.

The challenges of minimally invasive surgery are further complicated by the goal of avoiding *cardiopulmonary bypass*. In this procedure, a perfusion machine replicates the function of the heart and lungs so that *cardioplegia* can be used to safely stop the heart. The inflammatory response and postoperative infection associated with cardiopulmonary bypass is currently believed to be worse than the morbidity caused by sternotomy (Mack 2001; Ascione et al. 2000). Avoiding this morbidity requires surgery on the beating heart, which greatly increases the difficulties involved in precise manipulation and worksite access (Borst and Gründeman 1999). Instrumentation is required that can provide stable manipulation of an arbitrary location on the *epicardium* (surface of the heart) (Zenati 2001). Local mechanical immobilization of the epicardium is the approach generally followed using endoscopic stabilizers such as the Endostab device and the endo-Octopus device (Falk 1999; Gründeman 2003), which operate with positive pressure or suction. However, the resulting forces exerted on the heart can adversely affect its electrophysiological and mechanical performance. Care must be taken in order to avoid *hemodynamic* impairment (mechanical circulation problems) or life-threatening *arrhythmia* (alteration in the heartbeat rhythm) (Falk et al. 2000). As an alternative, several researchers in robot-assisted endoscopic surgery are investigating active compensation of heartbeat motion by visually tracking the epicardium and moving the tool tips accordingly (Çavusoglu 2003; Ortmaier 2003; Ginhoux 2004), but this research problem remains open. The motion of the beating heart is complex. In addition to the challenges of modeling or tracking the heart surface, active compensation will require considerable expense for high-bandwidth actuation to manipulate in at least 3 degrees of freedom over a relatively large workspace (Çavusoglu 2003).

1.2 The HeartLander Concept

These problems are avoided with the HeartLander system. Rather than attempting to stabilize the surface of the heart with respect to the stationary reference frame of a table-mounted robotic device, we propose that the robot be mounted directly in the moving reference frame of the beating heart (Figure 3). A miniature mobile robotic device will enter the chest through a minimally invasive port, attach itself to the epicardial surface, and travel to the desired location for therapy. The problem of the adapting to beating-heart motion is thus avoided by attaching the device directly to the epicardium. This allows cardiopulmonary bypass to be avoided without requiring mechanical stabilization of the epicardium. The ability of the robot to crawl to any location on the heart from a single starting point resolves the problem of operative site limitation. The mobility also allows HeartLander to reach multiple operative fields from a single incision, and thus making the insertion location independent of the operative site location for the procedure. For the teleoperated manipulator systems, the insertion planning for the tools is critical to the location of the operative field, and must be performed using an intercostal transthoracic approach. Alternatively, the independence of the insertion point for HeartLander allows the use of a *subxiphoid approach*. Using this technique, direct access to the heart is gained through a single incision is made below the sternum. The major advantage of the subxiphoid approach is that it not only obviates sternotomy, but avoids entering the pleural space altogether. As a result, deflation of the left lung is no longer needed and it becomes feasible to use local or regional rather than general anesthetic techniques. This has the potential to open the way to ambulatory outpatient cardiac surgery (Zenati et al. 2001).

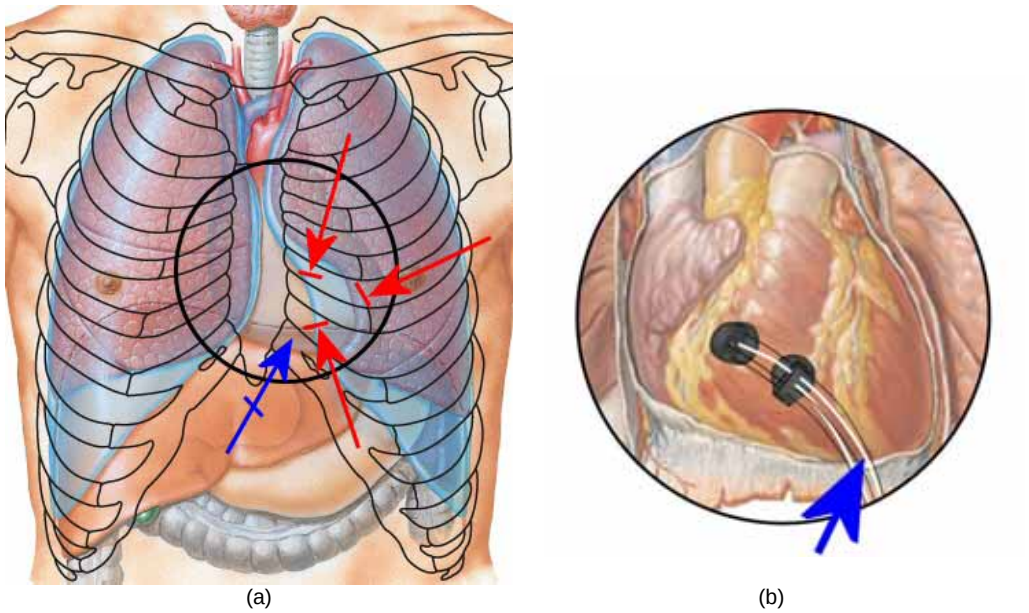

(a) (b)

Figure 3 . (a) Illustration of the HeartLander concept: the incision and insertion path for a subxiphoid approach *(blue line segment and blue arrow)*, and the incisions and insertion paths for an endoscopic approach *(red line segments and red arrows)*. Note that the endoscopic insertion paths pass through the pleural space *(light blue)*, while the subxiphoid path does not. (b) Close up of HeartLander on the epicardial surface of the heart.

There is a considerable number of both established and innovative procedures that could conceivably be performed entirely within the *pericardium* (the thin-walled sac that encloses the heart). This means that they do not intrinsically require access to the pleural space or areas outside the pericardium. Examples include:

- cell transplantation (Li et al. 1999);
- gene therapy for angiogenesis (Losordo, Vale, and Isner 1999);
- epicardial electrode placement for resynchronization (Leclercq and Kass 2002);
- epicardial atrial ablation (Lee et al. 1999);
- intrapericardial drug delivery (Gleason et al. 2002);
- ventricle-to-coronary artery bypass (VCAB) (Boekstegers et al. 2002).

Minimally invasive instrumentation is not currently available for most of these procedures, and those that do exist are typically designed for intercostal transthoracic access. However, all of these procedures could be performed without deflating the left lung if suitable instrumentation were available. These procedures would all benefit from the increased minimally invasive nature of HeartLander, and are thus be considered for initial therapeutic applications.

Table 1. Properties of the robotic teleoperative manipulator systems compared to those of the HeartLander system.

	Teleoperated Manipulators	HeartLander
Degrees of freedom	6	3
Dexterity	high	moderate
Number of incisions	3-6	1
Operative site availability	anterior surface	total heart
Tool reinsertion to change sites	yes	no
Lung deflation required	yes	no
Epicardial stabilization required	yes	no
Cost	$1,000,000	$10,000
Disposable therapeutic parts	no	yes
Cardiac surgical applications	all	intrapericardial

2 Design Concepts

This section describes the development of the broad conceptual design of the HeartLander system. Specifically, general methodologies for prehension, locomotion, and visual feedback are considered based on the system requirements.

2.1 System Requirements

The design requirements for HeartLander were as follows:

- **insertion**: must fit through a 20-mm diameter port
- **prehension**: must remain attached to the epicardium
- **actuation**: must have the flexibility to travel unrestrictedly
- **locomotion**: must have effective locomotive capabilities
- **feedback**: must provide adequate visual feedback
- **control**: must use a standard computer interface and joystick
- **therapy**: must demonstrate intervention ability

Aside from the size limitation, there were no quantitative design guidelines. Experimentally measured values for anatomical parameters such as shear forces generated by heart motion and pericardial coefficients of friction were not readily available from the literature. Were these data available, the suction force required to remain attached to the epicardium and the forces required to travel beneath the pericardium could have been estimated. Instead, prehensile forces were estimated from surgical stabilizers that adhere to the epicardium, and high actuation forces were supplied for evaluation in initial testing.

2.2 Prehension

The most obvious method for adhering to the surface of the heart was to use suction force generated by a negative pressure. Suction has proven to be effective for epicardial prehension in mechanical surgical stabilizers such as the Octopus™ and Starfish™ (Medtronic, Minneapolis, MN). These devices are either used to hold a small area of the epicardium still for operation, or to reposition the heart to expose a region of interest. The FDA-approved devices operate in a pressure range of 200-400 mmHg (Knight, Fox, and Schulze 2002). Suction is also used in the design of traditional mobile robotics, such as robots that inspect the hulls of ships or climb walls (Siegel 1998; Backes, Bar-Cohen, and Joffe 1997; Chen and Yeo 2003).

As an interesting alternative technology, researchers are attempting to fabricate biologically inspired synthetic gecko foot hairs (Sitti and Fearing, 2003). They are developing arrays of spatulae or "hairs" mimicking those of the foot of the gecko; these form a dry adhesive—a sort of biomimetic "Velcro"—capable of adhering to almost any surface, wet or dry, smooth or rough. To date they have developed arrays of spatular stalks that exhibit adhesion of 0.5 N/cm^2 (Campolo et al., 2003). However, they aim to achieve 10 N/cm^2. When this technology matures, it may prove a viable alternative to suction.

2.3 Actuation

Because HeartLander must be able to travel to any area on the heart from the starting location, the tether of the robot must be as flexible as possible. A design using onboard motors would require only thin wires for transmission of power and motor signals. Although this would have resulted in the most flexible tether, several other considerations eliminated its use. A search of commercially available miniature motors is summarized in the table below. The smallest motors (DC Micro, Smoovy), may have fit within the size restrictions, but delivered so little torque that it was believed that they would not be sufficient for locomotion on the tightly confined and volatile surface of the heart. The larger motors delivered substantially more torque, but would have been extremely difficult to incorporate into a design that fits within a 20-mm diameter. In addition to reducing the size and weight, using remote actuation allows the therapeutic portion of the robot to be extremely inexpensive, thus creating the possibility for the clinically disposable device. The absence of motors or electrical current on the portion of the robot that enters the patient may also lead to more expedient FDA approval.

To maximize the torque to size ratio, we chose remote actuation using external motors and a mechanical transmission running through the tether. The three transmissions considered were: flexible drive shafts, cable-driven, and wire-driven. Even the smallest, most flexible drive shafts proved too stiff to allow the tether curvature required to travel in an unrestricted manner on the heart. Traditional cable-driven transmissions require an antagonistic cable pair for each rotational degree of freedom, due to the fact that cables can support only tensile forces. This necessitates two cable pairs (i.e. four cables) to provide two rotational degrees of freedom. The ability of wires to support both tension and compression allows the same mobility to be provided using only three elastic wires, thus reducing the thickness and stiffness of the tether. Additionally, cable-driven transmissions require restorative elastic elements the shape against the tensile forces of the cable pairs. Because each wire is itself an elastic element, the wire-driven transmission does not require an additional restorative elements. For these reasons, a wire-driven transmission was selected for the method of remote actuation.

Table 2. Properties of several small motors considered for an onboard motor design.

	Diameter (mm)	Length (mm)	Weight (g)	Torque (μNm)
Smoovy – DC Micro	3	10.2	0.326	25
Faulhaber – DC Micro	6	20.15	2.0	113
Arsape – Stepper	6	14.65	1.4	200

2.4 Locomotion

The following subsections briefly outline the most promising potential locomotion designs that were considered.

2.4.1 Tank

This design moves in a manner similar to that of a tank, with two sets of rolling treads. Prehension is provided by suctions ports that are periodically located around the treads. These ports cycle ON/OFF as the treads turn. The ports along the bottom of the treads have suction ON. As the treads move a port away from the heart, the suction status changes to OFF to release the heart and maintain suction pressure in the other ports. This vehicle also turns in a manner similar to that of a tank, by stopping the tread on the side of the vehicle toward which to turn. Adapting to uneven terrain is achieved by using flexible treads.

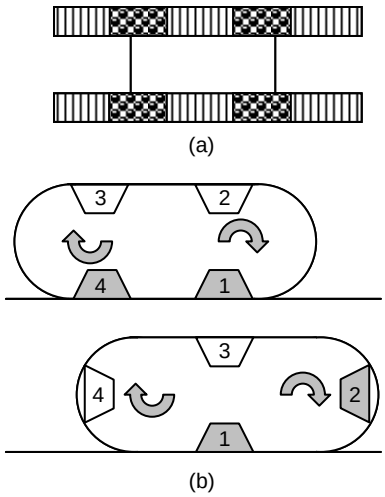

Figure 4 . (a) Bottom-view of tank design, circular pattern shows suction ports. (b) Side-view of tank design, active suction ports shown in grey.

Advantages

- smooth motion
- constant contact with epicardium

Disadvantages

- requires a drive shaft or onboard motor

2.4.2 Roller

This design has two translational degrees of freedom to move in a Cartesian coordinate system. Two sets of wheels with treads provide the contact forces for locomotion, while an outer perimeter of suction grid provides a normal force to keep the vehicle against the heart. The suction force is sufficiently small to allow sliding to occur during locomotion. Adapting to uneven terrain is possible if the body can flex about the Cartesian axes.

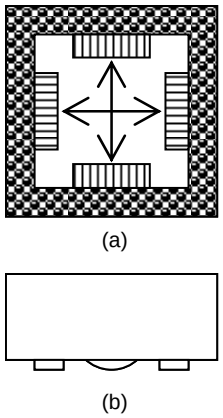

Figure 5 . (a) Bottom-view of roller design, circular pattern shows suction ports. (b) Side-view of tank design.

Advantages

- smooth motion
- constant contact with epicardium

Disadvantages

- poor adaptation to uneven terrain
- requires a drive shaft or onboard motor

2.4.3 Cartesian Walker

This design also has two translational, Cartesian degrees of freedom. Adapting to uneven terrain can be accomplished by adding passive compliant elements that angles the advancing foot downward, or by adding a rotational degree of freedom to control pitch.

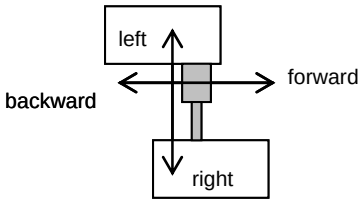

Figure 6. Top-view of Cartesian walker.

Advantages

- simple design and intuitive control

Disadvantages

- no yaw rotation
- step length dependent on body length

2.4.4 Polar Walker

This design has one rotational degree of freedom (yaw about the rear body section) and one translational degree of freedom (distance between the body sections). Adapting to uneven terrain can be accomplished by adding a passive compliant element to pitch the advancing body section downward, or by adding another rotational degree of freedom to control pitch.

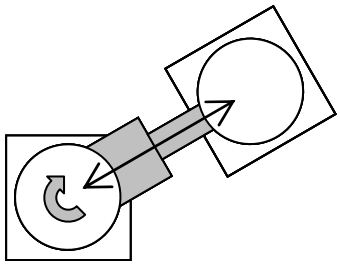

Figure 7. Top-view of polar walker.

Advantages

- simple and intuitive control

Disadvantages

- step length dependent on body length

2.4.5 Bending Inchworm Walker

This design has three degrees of freedom: two rotational and one translational. The lengths of the three elastic wires between the two body sections will determine the configuration based on minimum energy principles. The two rotational degrees of freedom allow yaw for steering and pitch to adapt to the surface curvature and uneven terrain. This design can also be implemented with antagonistic cable pairs and restorative elastic elements.

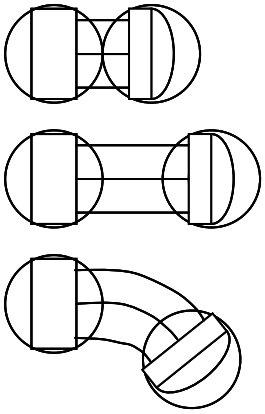

Figure 8. Top-view of bending inchworm extending and turning right.

Advantages

- simple design
- compact

Disadvantages

- more complex kinematics
- translation and rotation coupled

2.4.6 Final Selection

The bending inchworm walker was chosen for the HeartLander locomotive design due to the fact that it does not require a drive shaft and permits three degrees of freedom in a compact manner. The tank and roller designs both maintain constant suction contact with the epicardium and move in a smooth manner, but the constant motion of the tracks or wheels require the use a drive shaft. Since the smallest commercially available drive shafts were not flexible enough, these designs were eliminated. Of the three walker designs, both the Cartesian and polar walkers require sliding and/or rotating contact between components. The tolerances of these contacts must be carefully considered to avoid excessive friction or racking. Additionally, these moving components increase the size of the designs, especially if three degrees of freedom are provided. The bending inchworm design has three degrees of freedom, and no contact between moving parts. The three wires moving between the body sections, when properly constrained, determine the configuration of the device based on minimum energy principles. Therefore, the bending inchworm design permits three degrees of freedom in the most compact package, and the design is relatively simple to implement. For these reasons it was selected for the initial HeartLander locomotive design.

2.5 Video Feedback

Two possibilities were considered for the visual feedback system: (1) putting a small camera on the front body section, and (2) using fiber optics to transmit images from the front body to an off-board camera.

Using an onboard camera and transmitting the digital information back to the computer produces much higher image quality and increased tether flexibility. The smallest commercially available CCD camera found was the Panasonic GP-CX261V Color CCD Camera Module. The effective number of pixels for the sensor is 512(H) x 492(V), resulting in sufficiently high resolution (over 250,000 pixels). The CCD camera head has an 8-mm diameter and an 8.5-mm rigid length, and is disconnected from the much larger camera control unit (CCU) via a flexible printed circuit board (FPC) connector (Figure 10). Despite this feature, the camera head was still too large to meet our size restrictions. The incorporation of a lens would have further increased the size of this vision system and required optical engineering. Additionally, the length of the FPC extension (85 mm) was too short to allow the large CCU to be located outside of the patient. Panasonic engineers informed us that further extending the FPC would have deleterious effects on the image quality, and that an outside engineering firm would have to attempt it.

It is clear that CCD camera technology can be much further miniaturized without compromising image quality because of currently available medical videoscopes for endoscopy. These instruments have a camera located at the distal tip to ensure the highest image quality for diagnostic inspection of internal organs and structures. The Olympus BF-3C160 Bronchovideoscope measures 3.8 mm in diameter, which includes a 1.2-mm diameter working channel and fiber optic light

source. This implies that the CCD camera head has been fit into a space no larger that 2.6 mm in diameter. While these vision systems are not useful for our application due to their high cost and proprietary technology, they do illustrate the potential of using a CCD camera on HeartLander in the future.

Fiber optic image bundles provide much lower image resolution and increase tether stiffness, but can be very small in diameter and are relatively inexpensive. These fiber scopes also include a lens, light guides, and protective covering. We selected the FS-066-24 (ScopeTechnology, CT), which had the smallest available diameter (1.8 mm) in order to maximize the flexibility. Unfortunately, this also resulted in the smallest number of fibers in the optical bundle (6,000) and thus the lowest resolution.

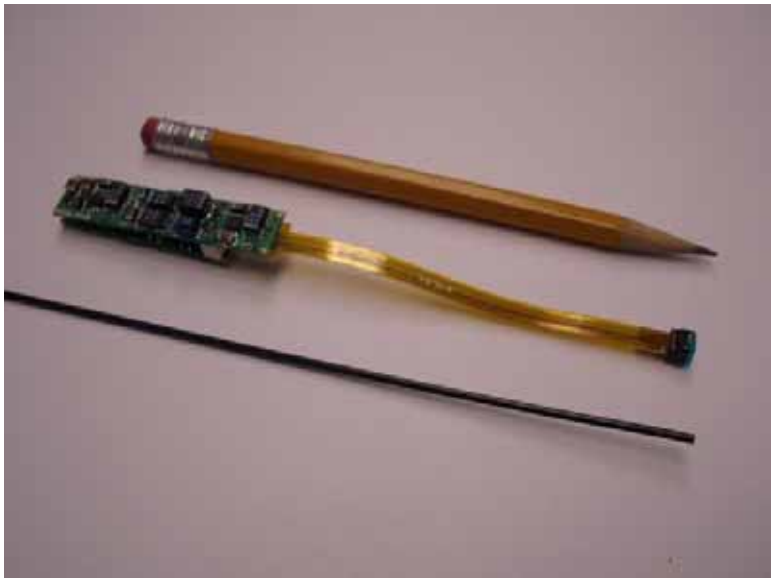

Figure 9. The vision systems: 1.6-mm fiber optic scope with light guide (*front*), the Panasonic GP-CX261V Color CCD Camera Module (*middle*), and a standard pencil for scale.

3 Design Implementation

This section describes the implementation details of the conceptual design that was developed in the preceding section. The HeartLander system consists of a crawling robot that is connected to supporting tabletop instrumentation via a tether (Figure 11). The tether transmits the functionality of the large external instrumentation required for prehension, actuation, vision, and control to the crawler. This design allows the therapeutic portion of the robot to be compact, lightweight, passive, and inexpensive. An initial prototype has been designed and constructed, the details of which are now further described (Patronik, Riviere, Zenati 2004b).

Figure 10. The control box *(upper left)*, motor box *(lower left)*, vacuum pump *(upper right)*, and tethered crawling robot *(lower right)*.

Table 3. The components and model specifications for the supporting instrumentation.

	Model
Computer	Dell
Monitor	Dell
Vacuum Pump	Starline
Video Camera	Sony
Light Source	Scope Technology, FO-150(Watt)
Control Box	
Power Supply	24VDC
DAQ Card	Iotech, DBK 202
Solid-State Relays	Opto22, G4 ODC5MA
Motor Box	
Motor Drivers	GeckoDrive, G201, 10µ Step
Motors	US Digital, size 23 stepper
Pressure Sensors	All Sensors, 15PSI-G-4V
Solenoid Valves	KIP Inc, 24VDC, 5/64 x 5/64

3.1 Supporting Instrumentation

The supporting instrumentation provides user input and functionality to the HeartLander robot. This instrumentation includes a joystick, computer, monitor, control box, motor box, vacuum pump, video camera, and light source (Table 3). The user input from the joystick is read by the HeartLander software, and the appropriate command signals are transmitted through the DAQ card in the control box. The DAQ card generates analog voltage signals for the three motor drivers, and digital voltage signals for the two solid-state relays. The motor drivers control the three stepper motors, which actuate the crawling robot through the mechanical transmission (see Section 3.2). The solid-state relays regulate the 24VDC power supply that switches the two solenoid valves. These 3-way valves connect the suctions pads of the crawling robot to either open air (OFF) or the vacuum pump (ON) through suctions lines that run through the tether. Pressure sensors are attached to each of the vacuum lines in the control box. The voltage signals from these sensors are read by the software through the DAQ card and used during locomotion (see Section 3.3). Images from the front module are transferred to an external video camera though a fiber optic scope in the tether. The digitized images from the video camera are then displayed on the monitor to provide visual feedback to the user. The fiber optic scope also transmits light from an external light source to the distal tip for illumination of the heart surface. By reading inputs from the user and pressure sensors and controlling the motor drivers and relays, the software orchestrates the locomotion of the crawling robot.

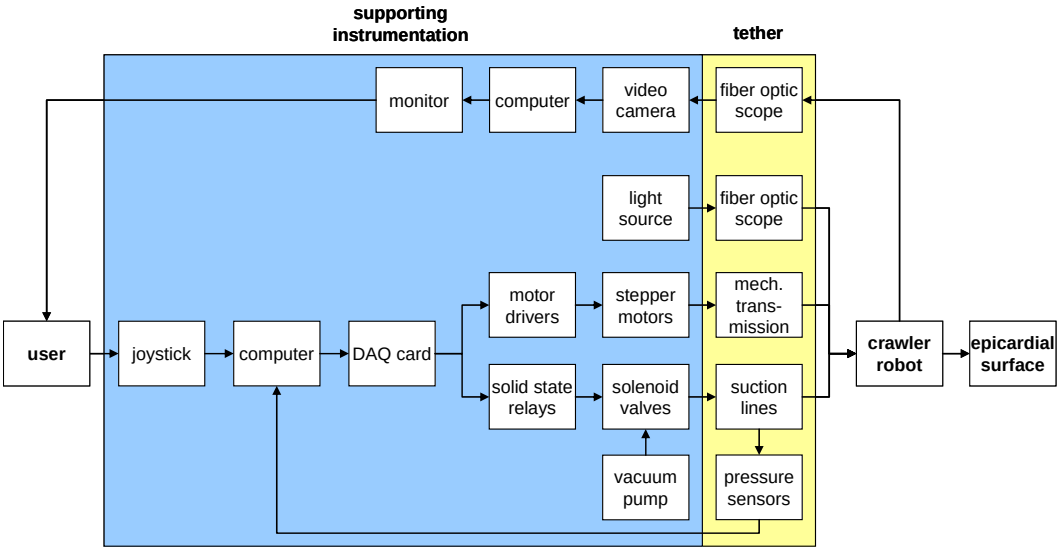

Figure 11. Flow chart of the HeartLander system. The user interacts with the supporting instrumentation *(blue block)*, which controls the crawling robot through the tether *(yellow block)*. Visual feedback is supplied back through the tether and supporting instrumentation to the user.

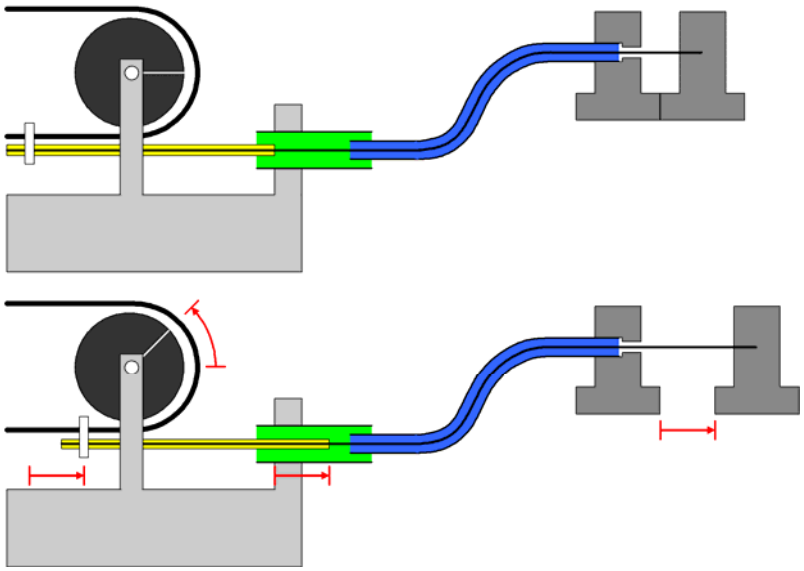

Figure 12. Illustration of mechanical wire transmission. Shown are: the pulley *(dark grey)*, the stationary motor assembly *(light grey)*, the reinforced wire *(yellow)*, the wire sheath *(blue)*, the wire *(heavy black line)*, and the body sections *(medium grey)*. *(top)* The wire is pulled back, drawing the body sections together. *(bottom)* The wire is advanced, pushing the body sections apart.

3.2 Mechanical Transmission

The mechanical transmission changes the rotational actuation of the stepper motor to linear actuation of the wire between the body sections of the crawler robot (Figure 12). There are three identical transmissions that actuate the crawler robot, one of which is described below. The rotor of stepper motor actuates a pulley (*shown in black*) that is attached to the stationary motor assembly (*shown in light grey*) through a timing belt. The linear actuation of the motor belt is used to translate the most proximal portion of the wire, which is reinforced by a larger diameter support wire using heat shrink for bonding (*shown in yellow*). This allows the wire to be directly actuated by the motor belt without bending. The reinforced section of wire then enters a transition tube (*shown in green*) that is attached to the motor assembly using set screws, and to the wire sheath (*shown in blue*) using heat shrink. The transition tube guides the portion of the wire that is not reinforced into the sheath with minimal bending or kinking. Additionally, the transition tube provides a method to securely attach the extremely thin wire sheath to the motor assembly in a way that does not close the sheath channel. This ensures that the wire slides freely within the wire sheath. The sheath is then attached to the rear body section, while the wire is attached to the front body section. In this manner, the rotational position of the motor directly corresponds to the length of wire between the front and rear body sections. This mechanical transmission allows the sheath and enclosed wire to assume any shape between the motor assembly and the rear body module, thus allowing the tether to passively comply with the environment during actuation.

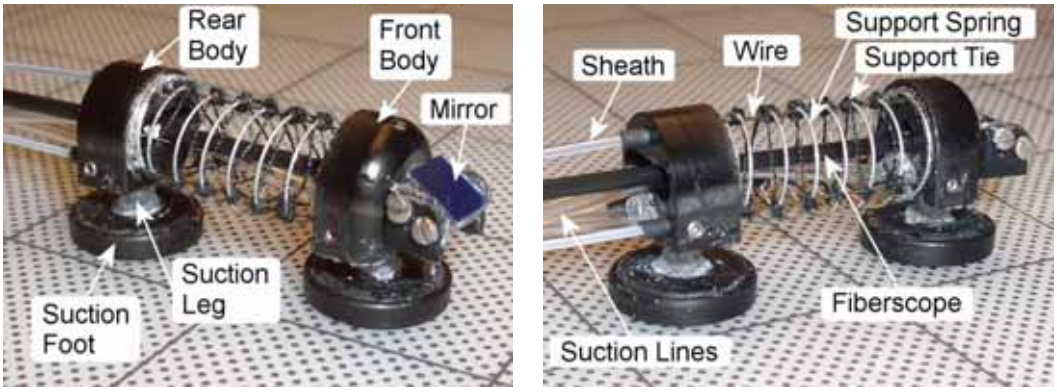

Figure 13. The crawling robot of the wire-actuated HeartLander prototype (*lines mark a 25.4-millimeter grid and the dots are spaced 2 millimeters apart*).

3.3 Crawler Robot

3.3.1 Construction

The crawling robot (Figure 13) consists of two body sections that can independently adhere to the epicardium and translate to produce locomotion. Each body section is mounted on a suction pad through a compliant suction leg. The compliance of the legs allows the pads to better adapt to the surface curvature and motion of the heart. The suction pads are independently supplied negative pressure through vacuum lines running through the tether to an external pump.

One translational and two rotational degrees of freedom are provided by three external stepper motors through the wire-actuated mechanical transmissions described in detail in Section 3.2. This design is a termed *continuum robot*, because it bends continuously along its length rather than at discrete joints (like the other walker designs from Section 2.4). The wires are radially located in 120° intervals, spaced 5 mm from the central longitudinal axis of the body sections. The super-elasticity of nitinol allows the use of small diameter wire (e.g. 0.15 mm) without causing permanent deformation. The elastic property of the wires also eliminates the need for additional shape-restoring components (e.g. springs or central elastic backbones) that are required in cable-driven transmissions. Low friction plastic (PTFE) is used for the wire sheaths to reduce the loss of force through the tether. A spring and several sets of uniformly separated support ties radially constrain the wires between the body sections, and thus prevent the wires from bowing outward during turning (Figure 14). A mirror is used to angle the view of the fiber optic scope toward the surface of the heart.

3.3.2 Kinematics

Determining the inverse kinematics of a continuum robot reduces to predicting the length and shape of the curve formed by the primary central backbone of the robot at any given time. In the case of the HeartLander crawling robot, the primary backbone is the extensible imaginary curve that passes through the center of the support spring between the rear and front bodies (Figure 15, *dotted line*). The HeartLander crawling robot is a single section of a traditional continuum robot due to the fact that forces are exerted along the backbone at only one point – the

front body section. In the absence of external forces, this means that the backbone curve will lie in a single plane known as the bending plane (Figure 15a, *shown in black*). The length of the backbone curve is simply the average of the lengths of the three wires, while the shape is that which minimizes the potential energy between the body sections generated by the boundary torques of the wires. If the weights of the bodies and friction between the wires and support spring are neglected, the minimum energy backbone curves will be circular (Gravagne and Walker 2000). These assumptions are valid for the current design and lead to a greatly simplified constant curvature kinematic model.

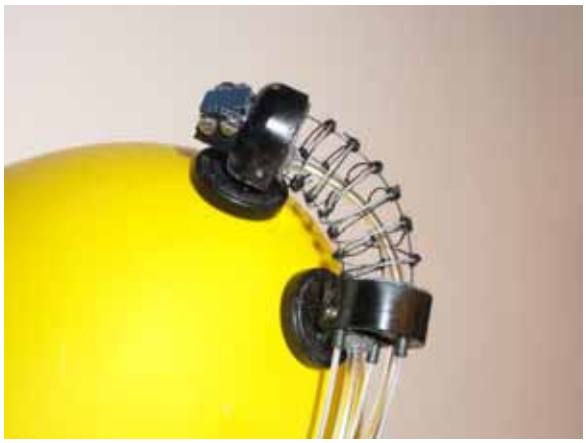

Figure 14. HeartLander prototype with spring to allow sharp turning without the wires bowing (*90˚ turn shown here*). Two rotational degrees of freedom allow the crawler to steer and conform to surface curvature.

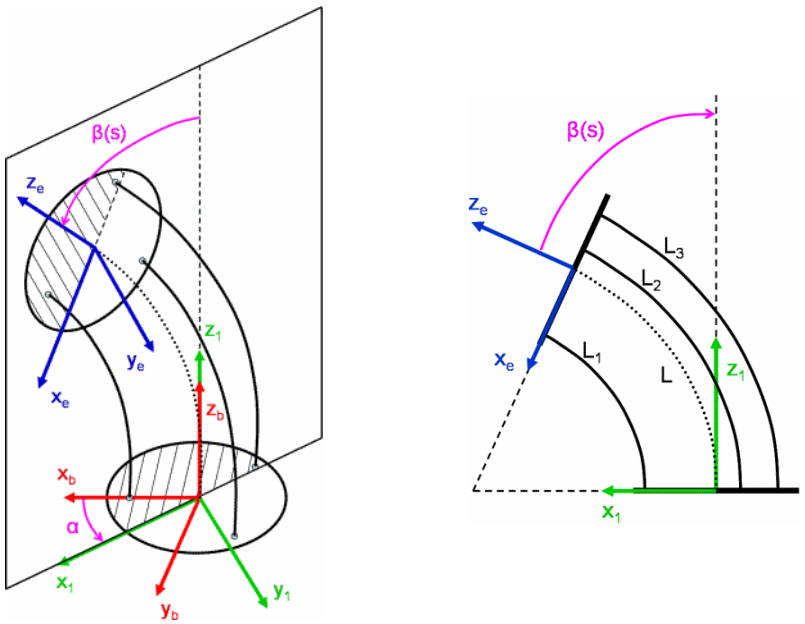

(a) (b)

Figure 15. (a) Kinematic diagram for the HeartLander crawler. Three reference frames are assigned: the base frame *(red)* attached to the lower body section, the bending frame *(green)* that is offset from the base frame by angle α, and the end frame *(blue)* that is attached to the upper body section. The bending plane *(black)* is defined by the angle α. The backbone bends angle β within the bending plane. (b) The base XZ-plane projection of the kinematic diagram. The lengths of the wires $(L_1\text{-}L_3)$ determine the configuration [α, β, L].

Three frames are used to define to the system. Recall that the wires pass freely through holes in the rear body section, and are anchored to the front body section. The **base frame** (*shown in red, subscript **b***) is attached to the rear body, with the *xy*-plane coincident with the wire thru holes and the *x*-axis intersecting the thru hole for wire 1. The **bending frame** (*shown in green, subscript **1***) is offset from the base frame by the **rotation angle** α about the collinear *z*-axes of both frames. The *xz*-plane of the bending frame is the plane in which the primary backbone will always lie, and is known as the **bending plane** (Figure 15a, *shown in black*). The orientation of the bending plane, and thus of the primary backbone curve, is completely defined by the rotation angle α. The **end frame** (*shown in blue, subscript **e***) is attached to the front body section, with the *xy*-plane coincident with the anchor points for the wires and the *x*-axis lying in the bending plane. The *z*-axis of the end frame is also contained within the bending plane, and the angle between it and the z-axes of the base and bending frames is known as the **bending angle** β. The primary backbone curve is completely defined by the length (*L(s)*), rotation angle (α), and bending angle ($\beta(s)$). In order to determine the entire set of points that constitute the backbone curve, length and bending angle are parameterized by a parameter (*s*) similar to arc length. If only the position and orientation of the end frame (i.e. front body) relative to the base frame (i.e. rear body) are desired, the parameterization can be dropped. Like the primary backbone, each wire bends within a single plane. These planes are parallel to each other and to the bending plane. Due to this fact, the lengths of the wires projected onto the bending plane are equal to the actual lengths of the wires. This allows the 3D problem to be reduced to the 2D projection into the bending plane (Figure 15b). The closed form solution to the inverse kinematics can be solved using simple geometry, and result in the following set of equations

$$L_i(s) = L(s) - \beta(s) \cdot r \cdot \cos\left(-\alpha + (i-1)\frac{2\pi}{3} \right) \qquad (1)$$

where L_i is the length of the wire between the body sections indexed by *i*, and *r* is the radius of the wires from the primary backbone.

3.3.3 Inherent Compliance

In the presence of external forces, the constant curvature model becomes invalid, and the shape of the backbone curve changes to minimize the potential energy of the system under the new force constraints. When the external forces are removed, the system returns to the constant curvature configuration without being damaged. This inherent compliance normal to the longitudinal axis is a general property of this class of continuum robots. While this property hinders tasks involving precise positioning of an end-effector, it gives continuum robots an advantage over discrete robots when navigating through time-varying environments (Hirose 1993; Gravagne and Walker 2000). In our application it allows HeartLander to safely contact and conform to the volatile surface of the heart without the need for expensive and complicated force feedback mechanisms.

4 Design Application

4.1 Insertion

A rigid subxiphoid videopericardioscope (SVP) will be used to access the heart and make a small opening in the pericardium (Zenati, Chin, and Schwartzman 2004). This device has a transparent conical tip that allows it to separate the intervening muscular and connective tissue of the diaphragm, thus clearing a direct path to the heart (Figure 4). This main channel contains an endoscope to visualize the insertion procedure. A second, inferior channel contains a grasper tool that is used to grab the pericardium and draw it back into the sharp edge of a cutting tool (Figure 4, inset). This passively makes an incision in the pericardium. HeartLander will then be inserted directly onto the epicardial surface through the SVP working channel, or through a port inserted after the SVP is extracted. Each body section of the crawling robot is 16 mm tall and has a 13-mm diameter circular footprint, thus allowing the device to pass through a 20-mm channel. Although this is too large for the current SVP working channel (7-mm diameter), future HeartLander prototypes versions will be made smaller and larger ports can be used in place of the SVP working channel. Once the treatment is complete, HeartLander will be retrieved by walking backwards or manually retracting the tether back through the port. Manual retraction also serves as the recovery method should the device become dislodged during the procedure.

4.2 Locomotion

The locomotion of HeartLander is a cyclic, inchworm-like process controlled by the supporting computer with input from a joystick interface. One cycle of the process is schematically illustrated in Figure 17a. During elongation, the front body is advanced by pushing the wires while the rear body is locked down via suction. During retraction, the rear body is advanced to meet the front body by pulling the wires after the suction grip is transferred from the rear to front body. This locomotion scheme requires that some amount of slack be maintained in the tether, and thus the tether must be made sufficiently long. Turning is achieved by differentially changing the lengths of the wires (Figure 17b). The seal at each suction pad is monitored using pressure sensors located in the supporting instrumentation. The control software ensures that at least one suction pad has a good grip at all times throughout the locomotive cycle. If the active suction pad does not achieve a good seal, likely due to the curvature of the heart surface, the software automatically adapts by "dithering" the position of the top center wire until a seal is formed.

Figure 16 . The subxiphoid videopericardioscopy (SVP) device inserted through a small subxiphoid incision *(circled)*. A surgical instrument (A) is being advanced through the working channel. The endoscope (B) and light supply (C) are visible. Inset shows a close-up of the distal end of the SVP. The upper channel is occupied by a 4-mm diameter endoscope enclosed by a conical transparent tip, while the inferior channel is open for use as a working channel. Shown here are the pericardial graspers (D) and cutting tool (E) for epicardial access [figure taken from Zenati, Chin, and Schwartzman 2004].

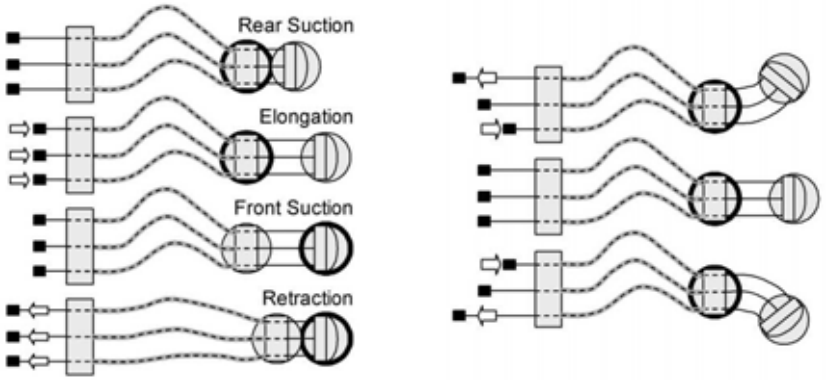

Figure 17. (a) Illustration of the locomotion cycle of the wire-actuated HeartLander prototype (*dark ring indicates the module that has active suction at each step of the process*). (b) Illustration of steering.

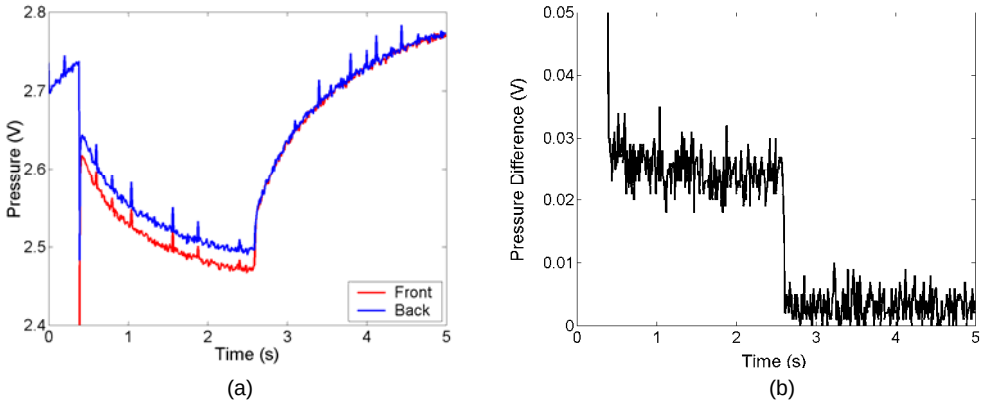

Figure 18. (a) The pressure signals from the front (red) and rear (blue) body sections. The drop at 0.5s occurs when suction is restored to the front suction pad, but there is no seal. The pressure drop from 0.5s to 2.5s continues while the front pad has no seal. At 2.5s, the front pad gets a seal with the heart surface and both pressure signals rise together. (b) The difference of the rear and front pressure signals, used to determine seal contact. A value greater than 0.015V shows that one pad does not have a seal, a value below 0.015V shows that both pads have a good seal.

4.3 Control

The HeartLander is controlled by the surgeon using a computer-based graphical user interface that provides video feedback. A joystick controls the direction and speed of travel (Figure 19). The previously described mechanical details of the locomotive process are completely controlled by the software, and thus are transparent to the surgeon.

The pressure from the front and back suction pads are constantly monitored by the software using the external pressure sensors. One typical cycle of the pressure readings is shown in Figure 18a. Initially, the rear pressure (*blue*) has suction contact with the surface, and the front pressure (*not visible*) is turned OFF while the front body section is being advanced. At 0.5 seconds, the rear pressure drops and the front pressure (*red*) increases when the front suction pad is turned ON. Both pressure signals then decay until 2.5 seconds. This indicates that both suction pads have suction turned ON, but that one does not have suction contact with the heart surface (in this case the front suction pad). At 2.5 seconds, the front suction pad also gets suction contact, causing both signals increase quickly, converge, then proceed to increase more slowly. The difference in the pressure signals is much greater when one suction pad does not have suction contact then when both have good suction contact (Figure 18b). Accordingly, the locomotion algorithm uses the pressure difference signal to rapidly ensure that both suction pads have suction contact before each elongation and retraction. The experimentally determined threshold value for the pressure difference was 0.015 V.

Visual feedback from the front body is relayed to an external video camera by a 1.6-mm-diameter flexible fiber optic endoscope running through the tether, and displayed to the user on the monitor (Figure 19).

4.4 Therapy

Therapy will be provided using existing endoscopic instrumentation deployed through the 3-mm working channel in HeartLander. In the future, dedicated end-effectors will be designed for more innovative therapies to be launched from the HeartLander platform.

Figure 19. The HeartLander control interface: joystick for control of locomotion, and monitor to display video from the device camera.

5 Testing

5.1 Bench Testing

Before testing on a beating animal heart, the HeartLander prototype was tested on flat chicken meat and a water-filled balloon.

5.1.1 Prehensile Testing with a Poultry Model

Bench tests using poultry breast were conducted in order to validate the pressure readings from the sensors and to estimate the prehensile forces that can be attained by the initial prototype. For all trials, only the rear body was supplied a vacuum pressure of 0.08 N/mm^2 (600 mmHg) by the pump. This pressure created a vacuum force (F_V) of 1.76 N between the suction pad and the surface of the poultry.

In the first test, a normal force (F_N) was applied upward on the rear body (illustrated in Figure 20a). The normal force required to break the suction contact was recorded using a digital force gauge (N=20), and the mean and standard deviation were calculated (Table 4). This force was also compared to the predicted vacuum force F_V.

In the second test, a tangential force (F_T) was applied to the rear body (illustrated Figure 20b). Again, the force required to break the suction contact with the surface was recorded using a digital force gauge (N=20). This force was also predicted from the vacuum force by balancing the moments about the edge of the suction pad using the following equation,

$$F_{T(predicted)} = \frac{F_V \cdot r}{h} \qquad (2)$$

where h and r are the elevation of the tangential force (10.12 mm) and the radius of the suction pad (5 mm), as depicted in Figure 20b.

For both the normal and tangential forces, the predicted magnitudes of the forces required to break the suction contact were close to the values measured with the force gauge, as shown in Table 4. A force of 2.01 N was required to remove the rear body using normal force, while a force of 0.86 N was required to break suction contact using tangential (i.e. shear) force.

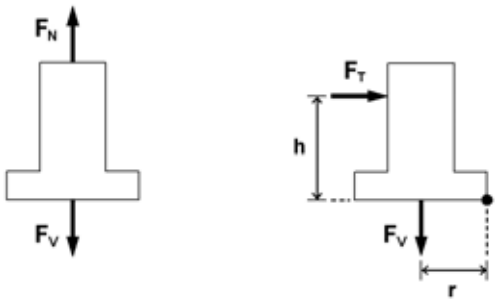

Figure 20. Free body diagrams of the rear HeartLander body section during tests to determine (a) normal force and (b) tangential force required to break suction contact with the surface of the poultry model.

Table 4. The means and standard deviations of the forces required to overcome the prehensile vacuum force created by a vacuum pressure of 600 mmHg (N=20, each).

Force	Mean (N)	Std. Dev. (N)
Normal (measured)	2.01	0.21
Normal (predicted)	1.76	0.01
Tangential (measured)	0.86	0.12
Tangential (predicted)	0.87	0.01

5.1.2 Manual Locomotion Testing with Poultry Model

Before the computer control of the HeartLander prototype was developed, the crawler and locomotion concept were tested on poultry breast (Patronik, Zenati, and Riviere 2004a). The wires were actuated using handles, and manual valves were used to switch the suction to the body sections (Figure 21a). The vacuum pump supplied the suction forces. The coordination between wire position and suction status for locomotion was verbally communicated between two operators. Although coordination was not efficient, the prototype was able to maintain prehension of the poultry breast and locomotion was demonstrated across several surfaces of the model (Figure 21b). These tests validated the locomotive design of the prototype, and illustrated the necessity of computer control.

5.1.3 Locomotion Testing with Balloon Model

In order to test the locomotive ability of HeartLander under computer control, walking trials on the surface of a water-filled balloon were performed. A standard latex balloon was inflated with water to a diameter of 9-cm, and coated with baby oil for lubrication. The user pressed forward on the joystick to initiate forward movement, but had no active role in adapting to the surface curvature of the balloon. The control software did not presume any surface curvature, and thus extended straight out initially for each step (Figure 22a). HeartLander was able to adapt to the balloon curvature and successfully travel across the balloon surface without any interaction from the user, aside from the joystick command to move forward (Figure 22). During some trials, the motion tether would cause substantial interference in the locomotion. In later animal trials with the pericardium intact, the small slit in the pericardium acted as a fulcrum to constrain the motion of the tether, thus obviating this problem.

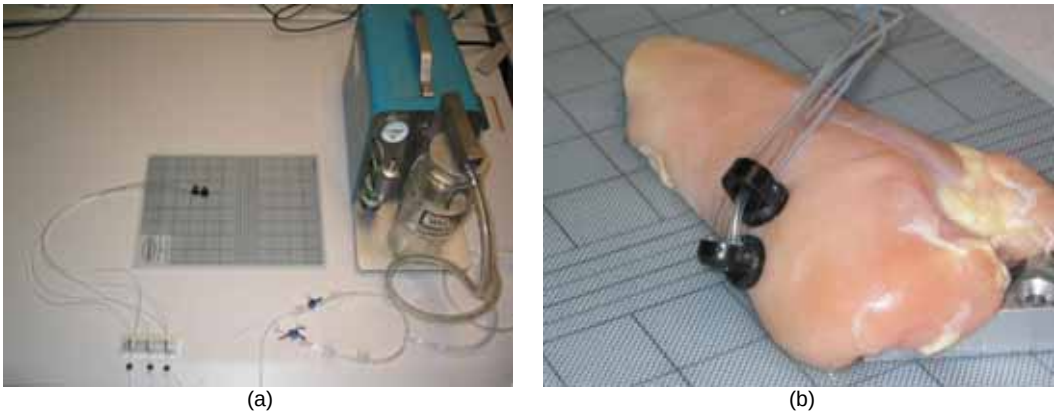

(a) (b)

Figure 21. (a) The setup for the poultry manual locomotion trials. Setup includes: wire-actuation handles *(lower left)*, manual valves *(lower right)*, vacuum pump *(upper right)*, HeartLander *(center)*. (b) HeartLander successfully walking over the curved surface of the poultry breast, raised with a block to generate curvature.

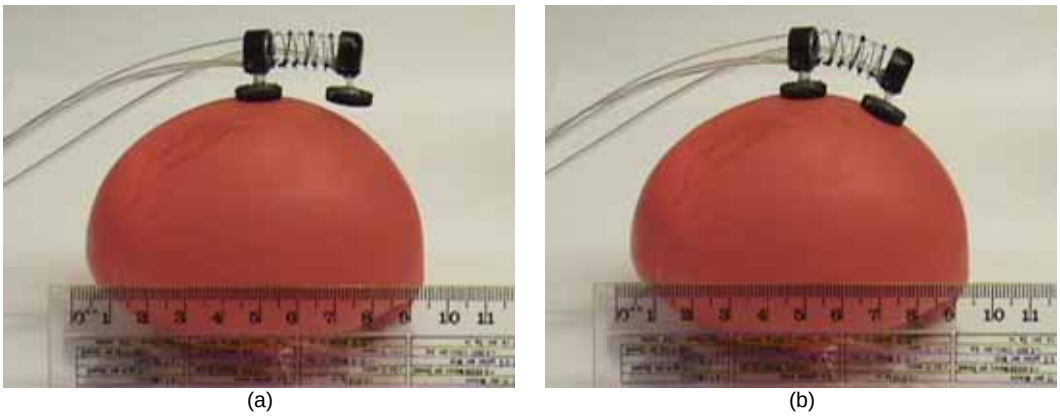

(a) (b)

Figure 22. Bench testing the locomotion algorithm traveling on a water-filled balloon lubricated with baby oil. (a) Pressure sensors indicate that advancing module does not have suction contact, (b) the middle wire is advanced, bending the front body downward toward the balloon surface until contact is made. *Ruler shows centimeter marks.*

5.2 *In Vivo* Porcine Testing

Three large (30-45 kg) crossbred swine were used for *in vivo* animal testing (Riviere, Patronik, and Zenati 2004). After standard single-lumen endotracheal intubation, a surgical plane of anesthesia was maintained using isoflurane, 1-3%. The animals were placed into supine position. Invasive hemodynamic and arterial blood gas monitoring was performed throughout the procedure. Median sternotomy was performed and the pericardial sac was opened. An apical suction positioner (Starfish^{TM}, Medtronic, Minneapolis, MN) was used to present various areas of the right and left ventricle at the center of the operative field. The HeartLander was manually placed on the epicardium at the start of each walking trial. Locomotion across the epicardial surface in various directions was tested for approximately 15 minutes in each trial.

Crawling on the epicardium was tested first on the anterior wall of the beating right ventricle (RV) in each animal. Locomotion in a straight line was successfully accomplished with the scope inserted through the HeartLander device. Figure 23 shows the visual feedback provided to the surgeon that proved sufficient to identify larger landmarks, such as the left anterior descending artery (LADA). As the epicardial curvature increased, however, the scope caused inconsistent epicardial prehension because the stiffness hindered the device in conforming to the shape of the heart. Subsequently, therefore, the HeartLander was tested without the scope inserted. A curved trajectory was successfully reproduced on the anterior RV and allowed crossing of the LADA) onto the anterior wall of the left ventricle (LV). No adverse hemodynamic or electrophysiologic events were observed during crossing over the coronary artery. No gross epicardial damage was observed along the trajectory of the HeartLander. Figure 24 presents a time sequence of photographs of the HeartLander as it walked across the epicardial surface of the heart *in situ*. The device can be seen to traverse a portion of the heart, crossing the LADA. This figure also shows the turning capability of the device.

Following anterior RV crawling with the heart left *in situ*, the Starfish device was applied to the apex of the LV and the beating heart was elevated and retracted laterally to the left as shown in Figure 25 in order to present the inferior wall of the RV at the center of the operative field. The HeartLander was manually applied to the anterior wall of the beating RV and remotely controlled to move inferiorly, crossing the acute margin of the RV onto the inferior wall. This task poses several challenges to the HeartLander, requiring crawling on diverse terrain with varying degrees of curvature and requiring several changes of direction in order to complete a curved path. The HeartLander successfully completed this experiment in all 3 animals. Occasional failures of the front foot to make good contact with the epicardium in areas around the acute margin were encountered in the first two subjects; these were eliminated in the last experiment by decreasing the length of the step.

The speed of travel in these experiments was approximately 8 cm/minute. The relatively high profile of the device did not allow access to other parts of the heart that were still covered by the pericardial sac.

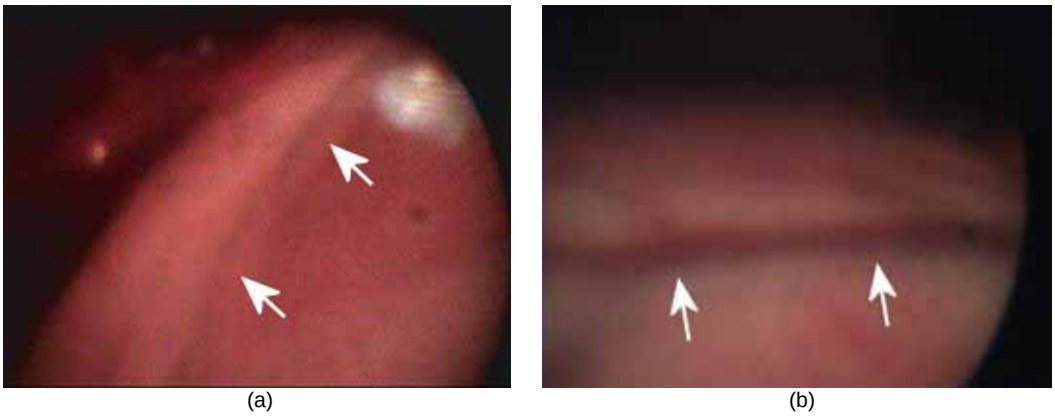

(a) (b)

Figure 23. (a) View of the left anterior descending artery (LADA) through the scope during approach (*arrows highlight*). (b) View of the LADA when the device is located directly above the vessel (*arrows highlight*).

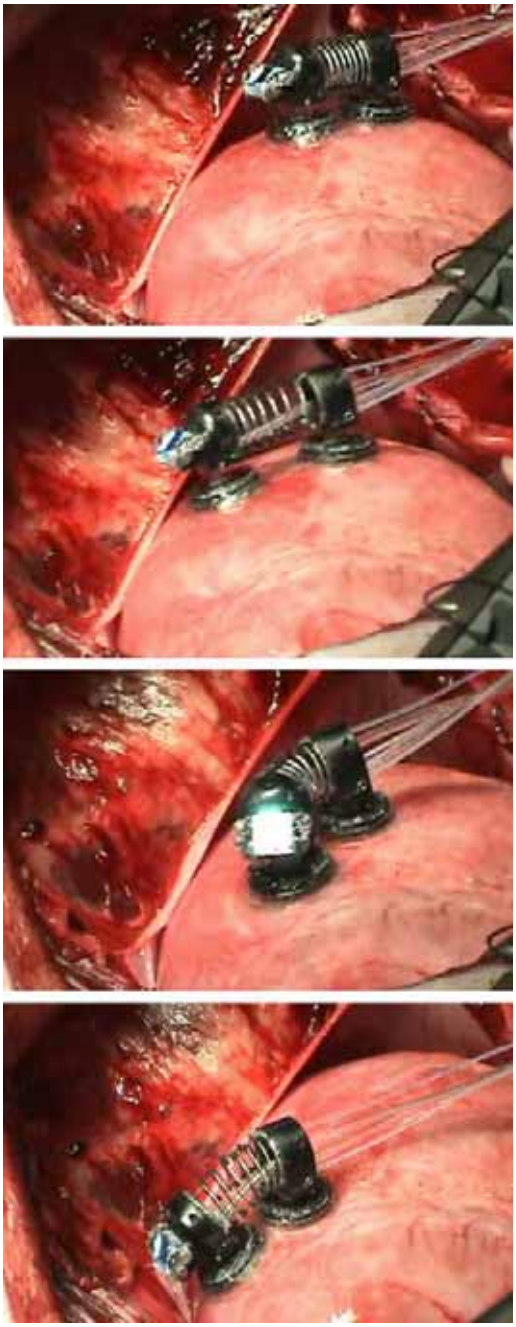

Figure 24. A time sequence showing the Heart-Lander traveling across the beating porcine heart *in situ*, starting from a point near the anterior wall of the right ventricle and ending near the acute margin. The third photograph (lower left) also shows the steering capability of the device.

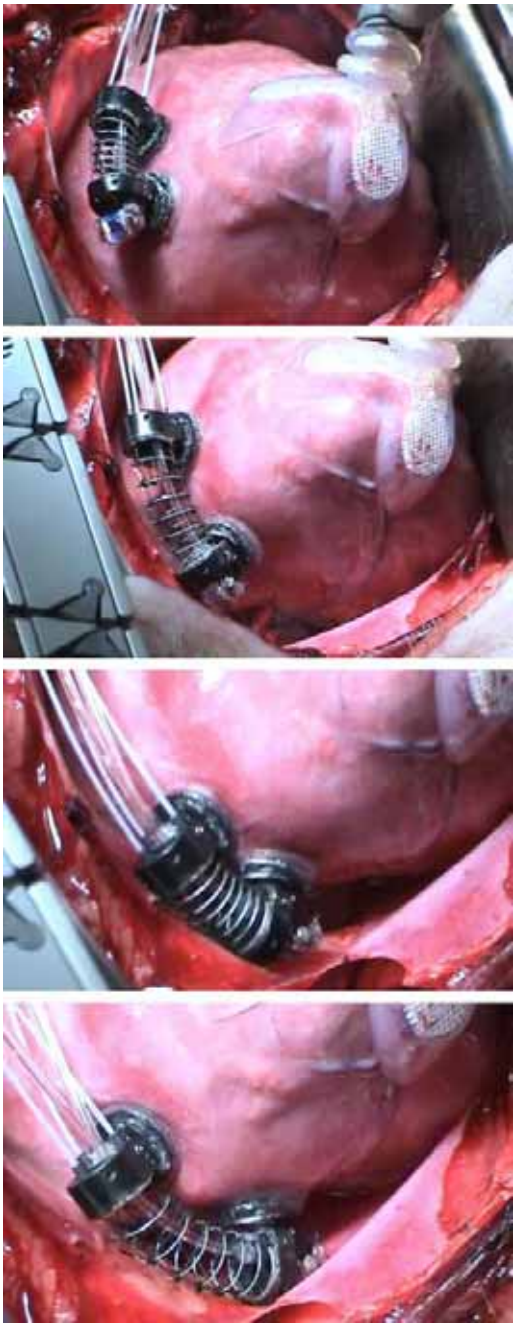

Figure 25. A time sequence showing the Heart-Lander traveling from the anterior wall of the RV, across the acute margin and onto the inferior wall of the RV of a beating porcine heart repositioned using the Starfish (Medtronic, MN).

6 Discussion and Future Work

The results presented in this report demonstrate the feasibility of using a mobile robot to adhere to and maneuver on the epicardial surface of a beating heart. This represents the first step toward the development of the HeartLander system to facilitate minimally invasive beating-heart intervention.

Future porcine tests will proceed from open-heart testing to minimally invasive testing using a subxiphoid approach. In order to facilitate operation in the space between the epicardium and pericardium, the profile of the next prototype must be greatly reduced. If tether stiffness due to the actuation wires continues to be a problem, an onboard motor design will be evaluated for comparison. Additionally, an alternative vision system must be incorporated to eliminate the severely deleterious effects of the fiber optic scope rigidity, and to improve the image quality for feedback to the surgeon. This will most likely be accomplished with the use of an onboard camera. Appropriate instrumentation to facilitate subxiphoid access must also be developed.

By employing a modular design for therapeutic end-effector attachment, HeartLander will be capable of performing a variety of surgical treatments. Prior to the development of these dedicated end-effectors, the 3-mm working channel will be used to deploy a variety of existing endoscopic tools from the stable HeartLander platform. The first application planned for evaluation is epicardial lead placement for resynchronization, using commercially available epicardial pacing leads (Leclercq and Kass 2002). As research continues, we plan to develop end-effectors for HeartLander for more innovative procedures, such as epicardial delivery of myoblasts or stem cells for regeneration of the failing myocardium. Ultimately, we envision adoption of HeartLander-based intrapericardial therapies not only by minimally invasive cardiac surgeons, but also by interventional cardiologists and electrophysiologists (Schweikert 2003; Sosa 2000).

References

Ascione R, Lloyd CT, Underwood MJ, Lotto AA, Pitsis AA, Angelini GD. 2000. Inflammatory response after coronary revascularization with or without cardiopulmonary bypass. *Ann Thorac Surg*. 69:1198-1204.

Backes, P.G., Bar-Cohen, Y., Joffe, B. 1997. The multifunction automated crawling system (MACS). *Proceedings., 1997 IEEE International Conference on Robotics and Automation*, 1: 335-340.

Boekstegers, P., Raake, P., Al Ghobainy, R., Horstkotte, J., Hinkel, R., Sandner, T., Wichels, R., Meisner, F., Thein, E., March, K., Boehm, D., Reichenspurner, H. 2002. Stent-based approach for ventricle-to-coronary artery bypass. *Circulation* 106:1000-1006.

Borst, C., Gründeman, P.F. 1999. Minimally invasive coronary artery bypass grafting: an experimental perspective. *Circulation* 99:1400-1403.

Bowersox JC, Cordts PR, LaPorta AJ. 1998. Use of an intuitive telemanipulator system for remote trauma surgery: an experimental study. *J Am Coll Surg* 186(6): 615-621.

Çavuşoğlu, M.C., Williams, W., Tendick, F., Sastry, S.S. 2003. Robotics for telesurgery: second generation Berkeley/UCSF laparoscopic telesurgical workstation and looking towards the future applications. *Industrial Robot* 30(1):22-29.

Chen, I.-M., Yeo, S. H. 2003. Locomotion of a 2D Walking-Climbing Robot Using Closed-Loop Mechanism: From Gait Generation to Navigation. *International Journal Robotics Research.* 22(1): 21-40.

Diodato MD, Damiano RJ. 2003. Robotic cardiac surgery: overview. *Surg Clin North Am*, 83(6): 1351-1367.

Falk V, Diegeler A, Walther T, et al. Endoscopic coronary artery bypass grafting on the beating heart using a computer enhanced telemanipulation system. Heart Surg Forum 2:199–205, 1999.

Falk, V., Diegler, A., Walther, T., Autschbach, R., Mohr, F.W. 2000. Developments in robotic cardiac surgery. *Curr Opin Cardiol* 15:378–387.

Ginhoux, R. Gangloff, J.A. de Mathelin, M.F. Soler, L. Arenas Sanchez, M.M. Marescaux, J. 2004. Beating heart tracking in robotic surgery using 500 Hz visual servoing, model predictive control and an adaptive observer. *Robotics and Automation, 2004. Proceedings. ICRA '04.* 1: 274 – 279.

Gleason, J.D., Nguyen, K.P., Kissinger, K.V., Manning, W.J., Verrier, R.L. 2002. Myocardial drug distribution pattern following intrapericardial delivery: an MRI analysis. *J Cardiovasc Magn Reson* 4(3): 311-316.

Gravagne I, Walker ID (2000) On the Kinematics of Remotely-Actuated Continuum Robots. IEEE Int'l Conf. on Robotics and Automation (ICRA), San Francisco, May 2000.

Gründeman PF, Budde R, Beck HM, van Boven W-J, Borst C. 2003. Endoscopic exposure and stabilization of posterior and inferior branches using the endo-Starfish cardiac positioner and the endo-Octopus stabilizer for closed-chest beating heart multivessel CABG: hemodynamic changes in the pig. *Circulation* 108:11-34.

Hirose S. Biologically Inspired Robots. Oxford Press, 1993.

Knight, G, Fox, WD, Schulze, DR. 2002. Cardiac stabilizer device having multiplexed vacuum ports and method of stabilizing a beating heart. U.S. Patent 6,589,166.

Leclercq, C., Kass, D.A. 2002. Retiming the failing heart: principles and current clinical status of cardiac resynchronization. *J Am Coll Cardiol* 39:194-201.

Lee, R., Nitta, T., Schuessler, R.B., Johnson, D.C., Boineau, J.P., Cox, J.L. 1999. The closed heart MAZE: A nonbypass surgical technique. *Ann Thorac Surg* 2:1696-1702.

Li, R.-K., Jia, Z.-Q., Weisel, R.D., Merante, F., Mickle, D.A.G. 1999. Smooth muscle cell transplantation into myocardial scar tissue improves heart function. *J Mol Cell Cardiol* 31:513-522.

Losordo, D.W., Vale, P.R., Isner, J.M. 1999. Gene therapy for myocardial angiogenesis. *Am Heart J* 138(2) Pt 2: S132-41.

Mack MJ. 2001. Minimally invasive and robotic surgery. *JAMA* 285(5): 568-572.

Ortmaier, T. J. 2003. Motion compensation in minimally invasive robotic surgery. Ph.D. dissertation, Technical University of Munich, Germany.

Patronik NA, Zenati MA, Riviere CN. (2004a) "Development of a Tethered Epicardial Crawler for Minimally Invasive Cardiac Therapies". *Proceedings of the IEEE 30th Annual Northeast Bioengineering Conference*. 2004; 239-240.

Patronik NA, Zenati MA, Riviere CN. (2004b) Crawling on the heart: a mobile robotic device for minimally invasive cardiac interventions. *Proceedings of the 7th International MICCAI Conference, Lecture Notes Computer Science*. 3217: 9-16.

Riviere CN, Patronik NA, Zenati MA (2004) A prototype epicardial crawling device for intrapericardial intervention on the beating heart. *Heart Surg Forum*, 7(6):E639-E643, 2004.

Schweikert, R.A., Saliba, W.I., Tomassoni, G., Marrouche, N.F., Cole, C.R., Dresing, T.J., Tchou, P.J., Bash, D., Beheiry, S., Lam, C., Kanagaratna, L., Natale, A. 2003. Percutaneous pericardial instrumentation for endo-epicardial mapping of previously failed ablations. *Circulation* 108:1329-1335.

Siegel, M., Gunatilake, P., Podnar, G. 1998. Robotic assistants for aircraft inspectors. *Instrumentation Measurement Mag*, 1(1):16-30.

Sosa, E., Scanavacca, M., D'Avila, A., Oliveira, F., Ramires, J.A.F. 2000. Non-surgical transthoracic epicardial catheter ablation to treat recurrent ventricular tachycardia occurring late after myocardial infarction. J Am Coll Cardiol 35:1442-1449.

Zenati M, Chin, A, Schwartzman D (2004) Subxiphoid videopericardioscopy: a new minimally invasive approach to the pericardial cavity for epicardial therapies. Proceedings of ISMICS 7th Annual Scientific Meeting, June 23-26, 2004; *Heart Surg Forum* 7(Supp. 1):S26.

Zenati MA, Paiste J, Williams JP, Strindberg G, Dumouchel J, Griffith BP. 2001. Minimally invasive coronary bypass without general endotracheal anesthesia. Ann Thorac Surg 72:1380-2.

Zenati, M.A. 2001. Robotic heart surgery. *Cardiol Rev* 9:287-94.